cmgh
CELLULAR AND MOLECULAR GASTROENTEROLOGY AND HEPATOLOGY

ORIGINAL RESEARCH

A Novel Mouse Model Harboring Hepatitis B Virus Covalently Closed Circular DNA

Zaichao Xu,[1,*] Li Zhao,[1,*] Youquan Zhong,[1,*] Chengliang Zhu,[2,*] Kaitao Zhao,[1] Yan Teng,[1] Xiaoming Cheng,[1,3,6] Qiang Chen,[4,5] and Yuchen Xia[1]

[1]State Key Laboratory of Virology and Hubei Province Key Laboratory of Allergy and Immunology, Institute of Medical Virology, School of Basic Medical Sciences, Wuhan University, Wuhan, China; [2]Department of Clinical Laboratory, Renmin Hospital of Wuhan University, Wuhan, China; [3]Wuhan University Center for Pathology and Molecular Diagnostics, Zhongnan Hospital of Wuhan University, Wuhan, China; [4]Department of Radiation and Medical Oncology, Medical Research Institute, Zhongnan Hospital of Wuhan University, Wuhan University, Wuhan, China; [5]Frontier Science Center for Immunology and Metabolism, Medical Research Institute, Wuhan University, Wuhan, China; and [6]Hubei Clinical Center and Key Laboratory of Intestinal and Colorectal Diseases, Wuhan, China

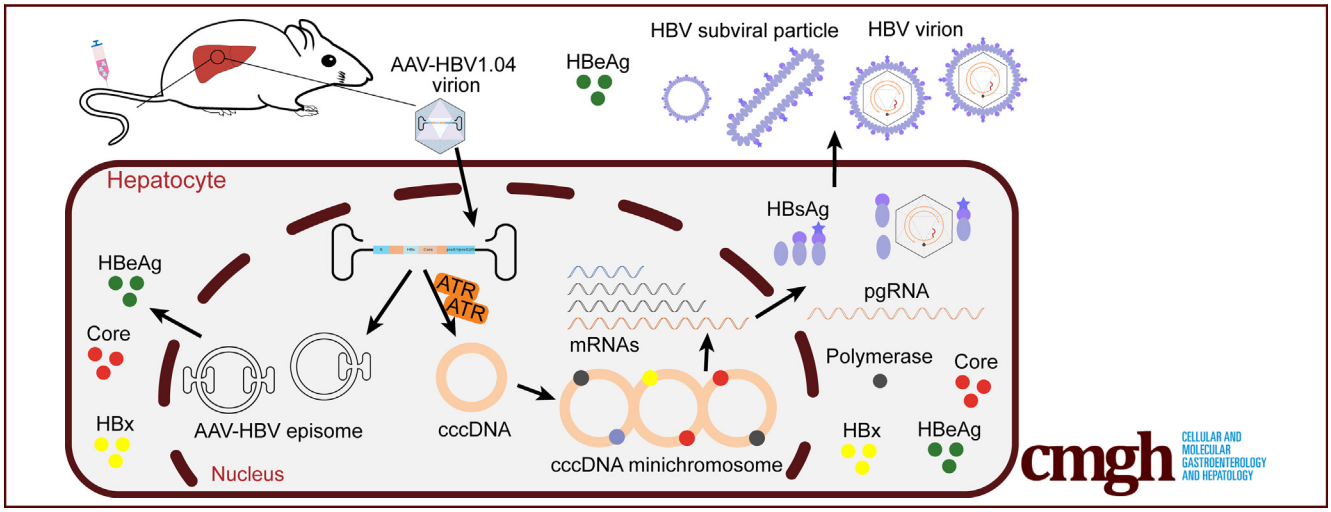

SUMMARY

By using an adeno-associated virus vector carrying a replication-deficient hepatitis B virus (HBV) genome, we established a mouse model harboring covalently closed circular DNA. This model provides a unique platform for studying HBV covalently closed circular DNA and developing novel antivirals to achieve HBV cure.

BACKGROUND AND AIMS: The persistence of viral covalently closed circular DNA (cccDNA) is the major obstacle for antiviral treatment against hepatitis B virus (HBV). Basic and translational studies are largely hampered due to the lack of feasible small animal models to support HBV cccDNA formation. The aim of this study is to establish a novel mouse model harboring cccDNA.

METHODS: An adeno-associated virus (AAV) vector carrying a replication-deficient HBV1.04-fold genome (AAV-HBV1.04) was constructed. The linear HBV genome starts from nucleotide 403 and ends at 538, which results in the splitting of HBV surface and polymerase genes. Different HBV replication markers were evaluated for AAV-HBV1.04 plasmid–transfected cells, the AAV-HBV1.04 viral vector–transduced cells, and mice injected with the AAV-HBV1.04 viral vector.

RESULTS: Compared with the previously reported AAV-HBV1.2 construct, direct transfection of AAV-HBV1.04 plasmid failed to produce hepatitis B surface antigen and progeny virus. Interestingly, AAV-HBV1.04 viral vector transduction could result in the formation of cccDNA and the production of all HBV replication markers *in vitro* and *in vivo*. The formation of cccDNA could be blocked by ATR (ataxia-telangiectasia and Rad3-related protein) inhibitors but not HBV reverse transcription inhibitor or capsid inhibitors. The AAV-HBV1.04 mouse supported long-term HBV replication and responded to antiviral treatments.

CONCLUSIONS: This AAV-HBV1.04 mouse model can support HBV cccDNA formation through ATR-mediated DNA damage response. The *de novo* formed cccDNA but not the parental AAV vector can lead to the production of hepatitis B surface antigen and HBV progeny. This model will provide a unique platform for studying HBV cccDNA and developing novel antivirals against HBV infection. *(Cell Mol Gastroenterol Hepatol 2022;13:1001–1017; https://doi.org/10.1016/j.jcmgh.2021.11.011)*

Keywords: HBV; cccDNA; Adeno-Associated Virus; Immune-Competent Mouse; Antiviral.

Despite the availability of effective vaccine, hepatitis B virus (HBV) causes a major public health burden worldwide, with about 257 million people being chronically infected.[1] Chronic hepatitis B patients are at high risk of developing liver cirrhosis and hepatocellular carcinoma.[2,3] At present, 7 drugs have been approved for chronic hepatitis B treatment, including 2 forms of interferons (standard and pegylated interferon) and 5 nucleos(t)ide analogs (lamivudine, adefovir, telbivudine, entecavir [ETV], and tenofovir).[4] All these treatments are effective to some extent but rarely lead to a cure for HBV infection.

HBV infection is initiated via virus interaction with heparan sulfate proteoglycans,[5] which is followed by the binding of large envelope protein with sodium-taurocholate co-transporting polypeptide (NTCP).[6] After internalization, viral capsids are directed to the nucleus, where the HBV genomes are released. In the nucleus, relaxed circular DNA (rcDNA) is converted into covalently closed circular DNA (cccDNA), which can persist in the nucleus as a minichromosome and serve as a template for viral RNA transcription. Viral messenger RNAs are transported to the cytoplasm, where they are translated into viral proteins. Together with the viral polymerase, the pregenomic RNA is encapsidated within the newly formed capsid and reverse transcribed into progeny rcDNA. Mature nucleocapsids are then either directed to the multivesicular bodies pathway for envelopment with HBV envelope proteins or redirected to the nucleus to amplify the cccDNA pool. As the viral persistence reservoir plays a central role in HBV infection, HBV cccDNA is the key obstacle for a cure.

The lack of animal models has significantly hampered HBV basic research and drug development. Although the mouse is the best characterized and most convenient laboratory animal, it cannot be infected with HBV. Currently, several mouse models support HBV replication and chimeric mouse models harboring human hepatocytes with susceptibility to HBV infection are the only option for studying HBV using mice. Transgenic mice with 1.3-fold HBV genome were generated.[7] Viral vector–mediated transduction of HBV DNA in mice was established with adenovirus or adeno-associated virus (AAV).[8,9] In addition, hydrodynamic injection of HBV plasmid via the tail vein allows the replication of HBV in the livers of immunocompetent mice.[10] In order to mimic the full life cycle of HBV infection, immune-deficient mice transplanted with primary human hepatocytes were used.[11] Moreover, liver and hematopoiesis double-humanized mice models were generated to investigate the crosstalk between HBV infection and immune response.[12] Although significant progresses have been made in establishing HBV mouse models, current models are still limited by inauthentic viral life cycle, difficulties in generation, high cost, and suboptimal immune response upon HBV infection.

As HBV cccDNA is not naturally formed in mouse hepatocytes, several cccDNA surrogate mouse models have been established. By using Cre/loxP-mediated DNA recombination or minicircle technology, mouse models with recombinant cccDNA-like molecules (rcccDNA) were generated.[13–16] Although the rcccDNA supports persistent viral replication and antigen expression, the nature of rcccDNA may differ from authentic cccDNA, as additional sequences, like LoxP or attR, were inserted into the HBV genome. Interestingly, it has been reported recently that HBV cccDNA can be detected in the liver of mice transduced with AAV-HBV.[17,18] However, how the cccDNA is formed and whether the cccDNA is functional in this model remain elusive. In this study, we took advantage of an AAV vector carrying a replication-deficient HBV1.04-fold genome (AAV-HBV1.04). Owing to the discontinuity of the S gene on the linear HBV genome, the AAV-HBV1.04 itself cannot express hepatitis B surface antigen (HBsAg) unless cccDNA is formed. After transduction of AAV-HBV1.04 into mouse, both HBsAg and cccDNA can be detected in the serum or liver, respectively. This novel mouse model will provide a unique platform for studying HBV cccDNA and developing novel antivirals to achieve HBV cure.

Results

Generation of a Replication-Deficient pAAV-HBV1.04 Vector

As in the previous AAV-HBV mouse model, all HBV replication markers could derive from both AAV-HBV vector or cccDNA, whether the newly formed cccDNA is functional remains uncertain.[17] To address this question, we generated an HBV replication-deficient pAAV-HBV1.04 vector. As shown in Figure 1*A*, the circular HBV genome was split from the S gene region to form a linear HBV genome. While the previously described pAAV-HBV1.2 construct contains all 4 major overlapping coding regions and expresses all HBV viral proteins, pAAV-HBV1.04 does not encode intact HBV polymerase and surface proteins. To validate its replication-deficient phenotype, we transfected Huh7 cells with pAAV-HBV1.2 or pAAV-HBV1.04 construct (Figure 1*B*). As expected, pAAV-HBV1.2 plasmid transfection resulted in the secretion of both hepatitis B e antigen (HBeAg) and HBsAg, whereas pAAV-HBV1.04 failed to express HBsAg (Figure 1*C*). In addition, HBV-DNA in the supernatant, which represents newly produced viral progeny, was not detected

***Authors share co-first authorship.**

Abbreviations used in this paper: **AAV, adeno-associated virus; ATM, ataxia-telangiectasia mutated; ATR, ataxia-telangiectasia and Rad3-related protein; cccDNA, covalently closed circular DNA; ChIP, chromatin immunoprecipitation; DDR, DNA damage response; DNA-PK, DNA-dependent protein kinase; dslDNA, double stranded linear DNA; ELISA, enzyme-linked immunosorbent assay; ETV, entecavir; HBc, hepatitis B virus core protein; HBeAg, hepatitis B e antigen; HBsAg, hepatitis B surface antigen; HBV, hepatitis B virus; NTCP, sodium-taurocholate co-transporting polypeptide; PBS, phosphate-buffered saline; Poly(I:C), polyinosinic-polycytidylic acid; qPCR, quantitative polymerase chain reaction; rcccDNA, recombinant covalently closed circular DNA–like molecule; rcDNA, relaxed circular DNA; SDS, sodium dodecyl sulfate; vg, viral genome.**

Most current article

2352-345X
https://doi.org/10.1016/j.jcmgh.2021.11.011

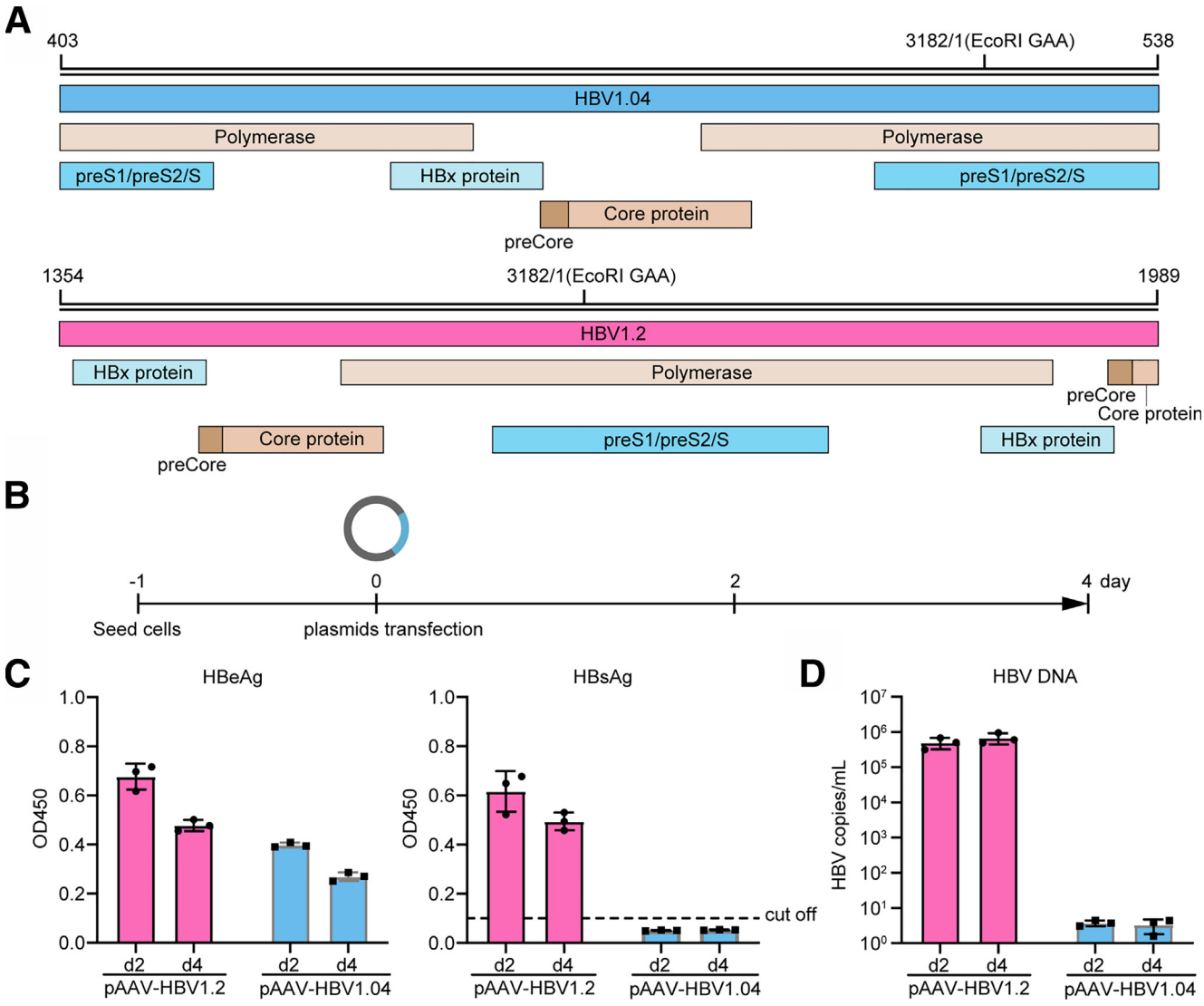

Figure 1. Construction and validation of pAAV-HBV1.04 plasmid. (*A*) Cloning of AAV vector with HBV1.04- and 1.2-fold genome. The HBV1.2 cassette allows the expression of all viral proteins, while the HBV1.04 cassette does not express intact HBsAg and polymerase. (*B*) Schematic representation of the experimental setting. Huh7 cells were transfected with pAAV-HBV1.04 or pAAV-HBV1.2 plasmid in 24-well plates, and the culture supernatants were harvested at 2 days and 4 days posttransfection. (*C*) The levels of HBeAg and HBsAg were determined by ELISA after 1:100 dilution. (*D*) HBV DNA was determined by qPCR. Data are presented as mean ± SD.

in pAAV-HBV1.04 plasmid–transfected cells (Figure 1*D*). These results confirmed that pAAV-HBV1.04 construct itself could not establish HBV replication.

AAV-HBV1.04 Transduction Results in HBV cccDNA Formation In Vitro

We next investigated whether AAV-HBV1.04 viral vector transduction was able to form cccDNA. AAV-HBV1.2 and AAV-HBV1.04 vectors were produced, titrated, and transduced into HepG2 cells or AML12 cells (Figure 2*A*). As shown in Figure 2*B*, both AAV-HBV1.2 and AAV-HBV1.04 transduction led to a significant increase of HBeAg over time in HepG2 cells. Interestingly, unlike direct plasmid transfection, HBsAg could be detected and increased gradually from AAV-HBV1.04–transduced cells (Figure 2*B*). Similar results could be observed on AML12 cells (Figure 2*C*).

To further validate the production of HBsAg, immunostaining was performed. As expected, AAV-HBV1.2–transduced HepG2 cells showed positive for both HBsAg and HBV core protein (HBc) (Figure 2*D*). In accordance with the enzyme-linked immunosorbent assay (ELISA) result, HBsAg could be detected in AAV-HBV1.04–transduced HepG2 cells by immunostaining (Figure 2*D*). The expression of HBsAg and HBc were further validated by Western blot (Figure 2*E*). Similar results were observed on AAV-HBV1.04–transduced AML12 cells (Figure 2*F* and *G*). As pAAV-HBV1.04 construct does not have an intact S gene, this result suggested that another HBV

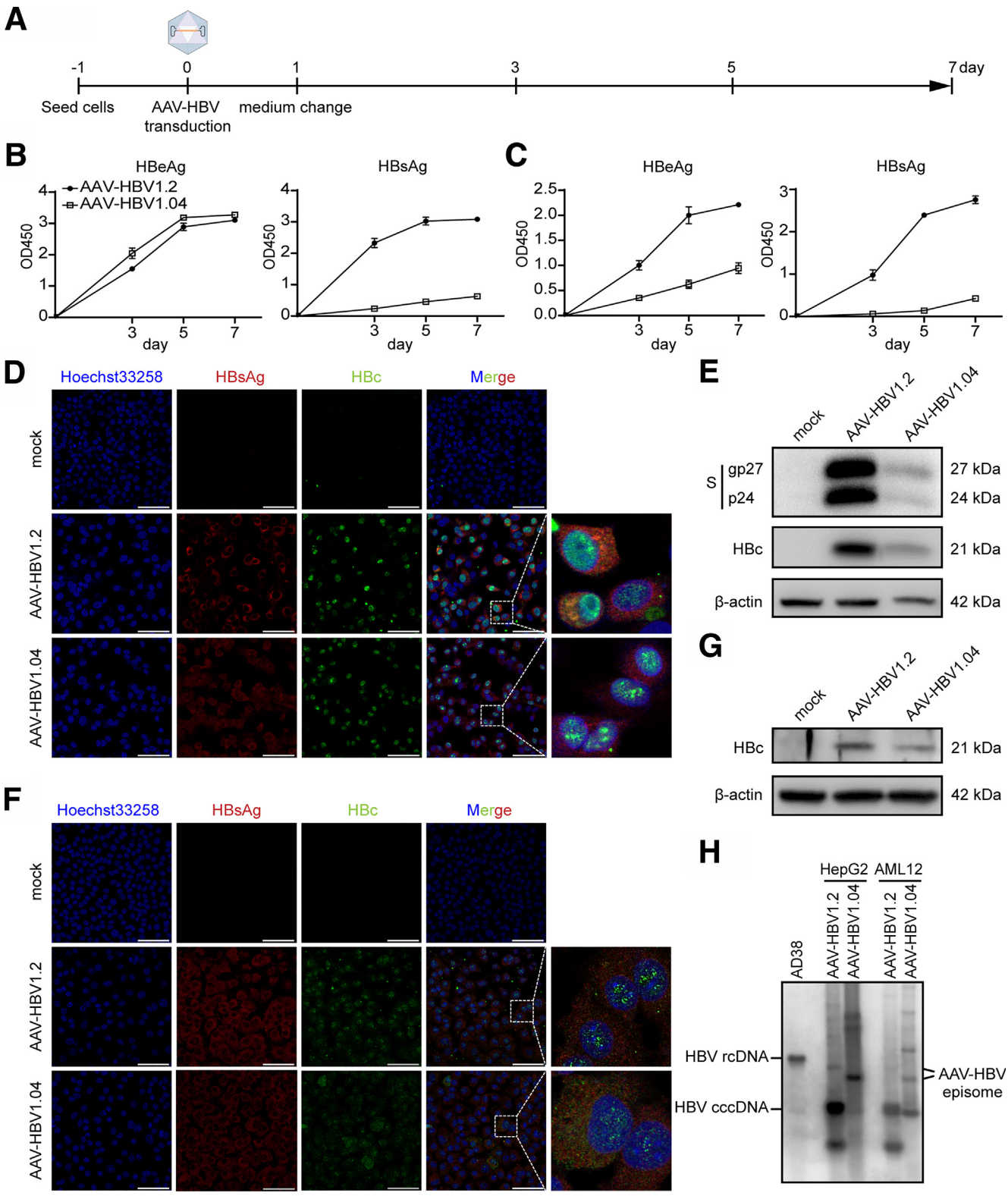

Figure 2. Detection of HBV markers in AAV-HBV1.04 viral vector–transduced cells. (*A*) Schematic representation of the experimental setting. HepG2 and AML12 cells were transduced with AAV-HBV at 5×10^4 vg per cell in 24-well plates. Secreted viral antigens in the supernatants of (*B*) HepG2 cells and (*C*) AML12 cells at different time points were determined by ELISA. (*D*) The levels of HBsAg and HBc protein in AAV-HBV–transduced HepG2 cells were evaluated by immunofluorescence staining. Scale bar = 75 μm. (*E*) The expression of HBc and HBs of AAV-HBV–transduced HepG2 cells was detected by Western blot. (*F*) The levels of HBsAg and HBc protein in AAV-HBV–transduced AML12 cells were evaluated by immunofluorescence staining. Scale bar = 75 μm. (*G*) The expression of HBc and HBs of AAV-HBV–transduced AML12 cells was detected by Western blot. (*H*) Cellular DNA was Hirt extracted and then subjected to Southern blot assay. Data are presented as mean ± SD.

transcription template, most likely cccDNA, was formed in this model. To test this hypothesis, cellular DNA was Hirt extracted and subjected to Southern blot analysis, the gold standard of cccDNA detection. Similar to previous report, different HBV DNA forms were detected in AAV-HBV–transduced cells.[17] Although owing to the different sizes of HBV genome inserts, the pattern of bands was different for AAV-HBV1.2 and AAV-HBV1.04, cccDNA could be detected in both groups (Figure 2*H*). Together, these results indicated that AAV-HBV1.04 transduction could support HBV cccDNA formation in cell cultures.

Ataxia-Telangiectasia and Rad3-Related Protein–Dependent DNA Repair Pathway Mediates cccDNA Formation

In the life cycle of HBV infection, cccDNA is formed through the conversion of rcDNA, which is either from the genome of input virion or from recycling of the newly formed nucleocapsid. To investigate whether cccDNA in this model is derived from rcDNA, cells were treated with different antivirals, including capsid inhibitors BAY41-4109 and GLS4, and reverse transcription inhibitor ETV 1 day after AAV-HBV1.04 transduction. Both capsid inhibitor treatments resulted in decreased HBc levels as expected (Figure 3*A*). Furthermore, BAY41-4109, GLS4, or ETV treatment led to suppressed HBV DNA (Figure 3*B*). However, HBsAg remained unchanged in all 3 groups (Figure 3*C*). Because HBsAg can only be generated from cccDNA in this model, these data suggested that the formation of cccDNA was not affected by these treatments. This interpretation was further confirmed by Southern blot (Figure 3*D*). Together, as BAY41-4109, GLS4, and ETV could block rcDNA synthesis but not cccDNA formation in this model system, our results implied that the cccDNA was formed through another mechanism.

AAV infection is known to induce host DNA damage response (DDR).[19] The activation of DDR kinases may result in the formation of cccDNA through AAV-HBV template. To explore this possibility, AAV-HBV1.04–transduced cells were treated with ataxia-telangiectasia mutated (ATM) kinase inhibitor (KU-55933), ataxia-telangiectasia and Rad3-related protein (ATR) inhibitors (AZD6738, VE-821) or DNA-dependent protein kinase (DNA-PK) inhibitor (KU-57788). While ATM kinase inhibitor and DNA-PK inhibitor only slightly affected HBeAg levels, 2 ATR inhibitors significantly decreased HBsAg levels (Figure 3*E*). As HBsAg could serve as a marker for HBV cccDNA in this model, this result suggested that ATR inhibitors may mitigate cccDNA formation. Next, we performed Southern blot to evaluate the effect of these DDR kinase inhibitors on cccDNA formation in this model. As shown in Figure 3*E*, in accordance with HBsAg ELISA results, 2 ATR inhibitors mitigated HBV cccDNA formation while the AAV-HBV episome remained unaffected (Figure 3*F*). Together, these data indicated that AAV-HBV1.04 viral vector transduction could result in HBV cccDNA formation through ATR-mediated DDR.

AAV-HBV1.04 Transduction Results in HBV cccDNA Formation and Long-Term Persistence In Vivo

We next tested if this AAV-HBV1.04 viral vector can be used to establish an HBV cccDNA mouse model. We injected mice with the recombinant AAV-HBV1.04 through tail vein and collected different samples at the indicated time points (Figure 4*A*). Results showed that serum HBeAg became positive right after injection and peaked after 8 weeks in both high-dose (5×10^{11} viral genome [vg]) and low-dose (5×10^{10} vg) groups (Figure 4*B*). HBsAg of the low-dose group showed similar kinetics as HBeAg, while HBsAg of the high-dose group reached the peak at 4 weeks after injection (Figure 4*C*). Serum HBV DNA could also be detected after injection (Figure 4*D*). The expressions of HBc and HBsAg were further determined by immunostaining, as shown in Figure 4*E*; more than 50% of the hepatocytes were positive for HBc and HBsAg 1 week after transduction. By Western blot, the expression of HBc could be detected 44 weeks after transduction (Figure 4*F*). The expression of HBc could only be observed in the liver, but not in other organs or tissues, suggesting that the AAV-HBV1.04 only targeted the mouse liver (Figure 4*G*). No obvious infiltrating lymphocytes or liver injury was observed 1 week after injection (Figure 4*H*).

We next evaluated the formation of HBV cccDNA in this mouse model. Southern blot revealed varied HBV DNA forms including HBV rcDNA, double-stranded linear DNA (dslDNA), AAV-HBV episome, and HBV cccDNA (Figure 5*A*). To further distinguish different HBV DNA forms in this mouse model, a previously described strategy combined with different enzymes digestion was applied.[17] Briefly, T5 exonuclease could digest linear and partial double-stranded forms of DNA; restriction endonuclease SacII could cut the AAV vector backbone thus linearize the AAV-HBV episome; the combination of both T5 exonuclease and SacII could digest all HBV DNA forms except cccDNA (Figure 5*B* and *C*). As shown in Figure 5*D*, Hirt-extracted DNA of HepAD38 cells showed 3 distinct bands including cccDNA, which is resistant to T5 exonuclease treatment. Similar to AAV-HBV1.2 transduction, a single band, which has the same size as cccDNA extracted from HepAD38 cells and could not be detected by the AAV-specific probe, was uncovered with the AAV-HBV1.04–transduced sample after T5 exonuclease and SacII treatments (Figure 5*D*). In addition, the presence of cccDNA was further verified by heating the sample to 85°C, which denatures rcDNA and dslDNA, but not cccDNA, into single-stranded DNA. As shown in Figure 5*E*, cccDNA from HepAD38, AAV-HBV1.2, or AAV-HBV1.04–transduced mouse liver is resistance to 85°C denaturation. Further treatment with EcoRI converted cccDNA into dslDNA (Figure 5*E*). Furthermore, Hirt-extracted AAV-HBV1.04–transduced samples were treated with T5 exonuclease and SacII, and the intact HBV cccDNA was confirmed by sequencing (Figure 6*A* and *B*).

To further examine whether HBV cccDNA generated in this model could resemble the cccDNA formed by natural HBV infection, the association of cccDNA with several

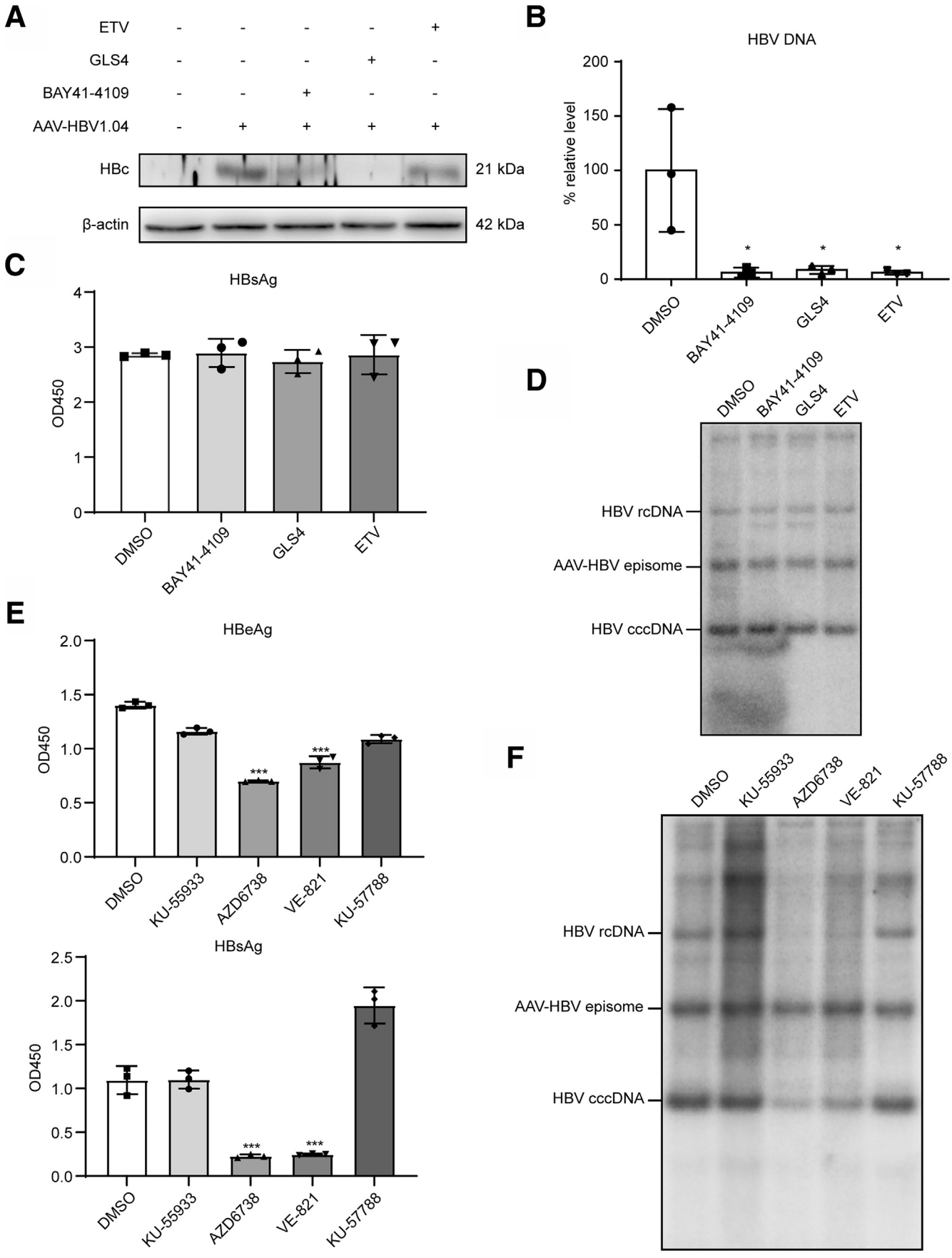
A
ETV
GLS4
BAY41-4109
AAV-HBV1.04
HBc
21 kDa
β-actin
42 kDa
B
HBV DNA
% relative level
DMSO
BAY41-4109
GLS4
ETV
C
HBsAg
OD450
D
HBV rcDNA
AAV-HBV episome
HBV cccDNA
E
HBeAg
KU-55933
AZD6738
VE-821
KU-57788
F

known cccDNA binding proteins was evaluated. Chromatin immunoprecipitation (ChIP) assays revealed that histone H3, HBc, and polymerase II were associated with cccDNA (Figure 6*C*). Together, these results suggested that the chromatinization and transcriptional activation of cccDNA formed in this model dose not differ from wild-type cccDNA formed through infection.

We next evaluated whether cccDNA could persist in the mouse liver. Southern blot of Hirt-extracted hepatic DNA revealed that cccDNA could be detected 44 weeks after AAV transduction in a dose-dependent manner (Figure 6*D*). Interestingly, HBsAg, HBeAg (Figure 7*A*), and HBc (Figure 7*B*) could be detected even 66 weeks after transduction, suggesting long-term persistence of HBV cccDNA in this model. Further, it was confirmed by Southern blot (Figure 7*C*).

AAV-HBV1.04 Mouse Model Is Suitable for Antiviral Evaluation

Next, we evaluated whether this AAV-HBV1.04 mouse model was suitable for studying antivirals against HBV. One week after AAV-HBV1.04 injection, mice were orally dosed with ETV everyday by gavage or injected intravenously with polyinosinic-polycytidylic acid [Poly(I:C)]. Mice treated in parallel with phosphate-buffered saline (PBS) served as control animals. Two weeks after treatments, different HBV replication markers were determined (Figure 8*A*). ETV, as a reverse-transcription inhibitor, is known to efficiently block HBV DNA synthesis but has little effect on cccDNA or viral proteins. As expected, ETV treatment clearly suppressed circulating HBV DNA but not HBsAg and HBeAg in the mice serum (Figure 8*B*). Inside the liver, ETV had no impact on HBV cccDNA, as demonstrated by Southern blot (Figure 8C). It did not change small HBs, HBc, and capsid as shown by Western blot (Figure 8*D*) but strongly suppressed capsid HBV DNA, as demonstrated by Southern blot (Figure 8*D*). When the mice were treated with Poly(I:C), all the tested HBV markers were strongly reduced, including HBsAg and HBeAg in the serum (Figure 8*E*), and small HBs, HBc, capsid, and capsid HBV DNA in the liver (Figure 8*F*). These results suggested that AAV-HBV1.04 mouse model is suitable for the evaluation of antivirals.

Taken together, we established a novel HBV mouse model that harbors cccDNA. This AAV-HBV1.04 mouse model could support HBV cccDNA formation through ATR-mediated DDR. While the AAV-HBV1.04 vector does not encode HBsAg and HBV polymerase, the HBsAg and HBV virion could only be generated from cccDNA. This model will provide a unique platform for studying HBV cccDNA and developing novel antivirals against HBV infection.

Discussion

While vaccine is available to prevent HBV infection, lifelong treatment is needed for chronically infected individuals. Complete sterilizing cure of hepatitis B, which is defined as undetectable HBsAg in serum and elimination of all forms of HBV DNA including cccDNA, can hardly be achieved.[4,20] The current aim of chronic hepatitis B treatment is a "functional cure." It is defined as seroclearance of HBsAg, undetectable serum HBV DNA, and normal liver enzymes and histology after stopping treatment, which requires complete blockade of HBV cccDNA.[4,20] As the key obstacle for HBV cure, cccDNA is a crucial target for antiviral treatment.[21] However, the narrow species tropism of HBV has greatly limited the development of animal models harboring cccDNA and hindered the progress of drug development. Chimpanzees are the only nonhuman primate fully susceptible to HBV infection.[22] Additionally, tree shrews can be experimentally infected with HBV.[23] Although the mouse is the best characterized and most convenient laboratory animal, it cannot be infected with HBV.

The identification of NTCP as an HBV receptor offers the opportunity to establish novel HBV infection models, including fully permissive immunocompetent HBV mouse models. Unfortunately, mouse NTCP cannot facilitate HBV entry.[24] Furthermore, mouse hepatocytes overexpressing human NTCP only support the infection of hepatitis D virus, while HBV infection, specifically cccDNA formation, remains restricted.[25] Additionally, cccDNA could not be established in HBV transgenic mice with high-level HBV replication.[7] These results indicated that HBV cccDNA cannot be formed in mouse hepatocytes through the conventional pathway as in human cells.

In the HBV life cycle, the formation of cccDNA requires capsid nuclear transportation, uncoating of rcDNA, and additional DNA repair processes. The detailed molecular events underlying the conversion of rcDNA to cccDNA remain elusive. Many evidences suggest that multiple steps have occurred, including release of the covalently bound viral polymerase and RNA primer from the respective negative- and positive-strand rcDNA templates, cleavage of terminal redundant sequence from the negative strand, repair of the incomplete positive strand, and ligation of both DNA strands.[26] The process may involve a bunch of host factors like flap structure-specific endonuclease 1, DNA polymerases, proliferating cell nuclear antigen, replication

Figure 3. (***See previous page***). **The formation of HBV cccDNA after AAV-HBV1.04 transduction.** AML12 cells were transduced with AAV-HBV1.04 at 5×10^4 vg per cell in 24-well plates. 24 hours post transduction, cells were treated with BAY 41-4109 (5 μM), GLS4 (0.2 μM), ETV (0.5 μM), or dimethyl sulfoxide (DMSO), and the cells were harvested at 7 days post-transduction. (*A*) The level of HBc was detected by Western blot. (*B*) HBV DNA from supernatant was determined by qPCR. (*C*) The level of secreted HBsAg was evaluated by ELISA. (*D*) Cellular DNA was Hirt extracted and then subjected to Southern blot. (*E*) One day after transduction, cells were treated with ATM kinase inhibitor (KU-55933, 5 μM), ATR inhibitors (AZD6738, 2.5 μM; VE-821, 2.5 μM), DNA-PK inhibitor (KU-57788, 5 μM) or DMSO for 5 days. Secreted viral antigens in the supernatant were detected by ELISA. (*F*) Cellular DNA was Hirt extracted and then subjected to Southern blot. Data are presented as mean ± SD, $^*P < .05$, $^{**}P < .01$ and $^{***}P < .001$.

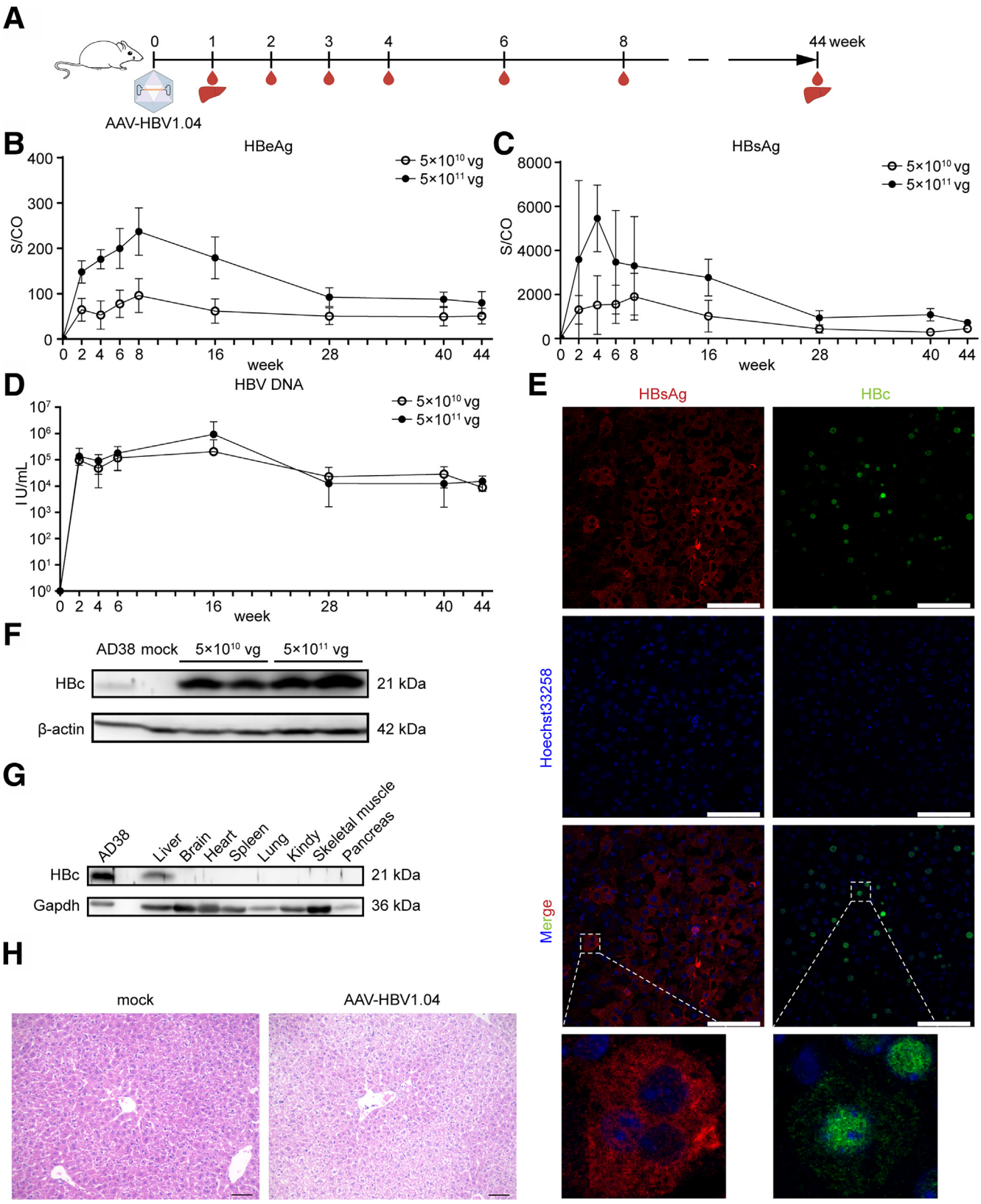

Figure 4. AAV-HBV1.04 transduction in vivo. (A) Female C57BL/6 mice (6–8 weeks old) were infected with AAV-HBV1.04 at 5×10^{10} or 5×10^{11} vg equivalents through tail vein injection. Samples were collected at the indicated time points. The kinetics of (*B*) HBeAg, (*C*) HBsAg, and (*D*) HBV DNA in mouse serum were evaluated. (*E*) Liver sections at week 1 posttransduction were collected for immunostaining of HBc and HBsAg. Scale bar = 75 μm. (*F*) Liver samples at week 44 posttransduction were collected to examine HBc by Western blot. (*G*) Different tissues from AAV-HBV1.04–transduced C57BL/6 mice at week 1 posttransduction were collected and HBc was tested by Western blot. (*H*) Liver sections from AAV-HBV1.04–transduced C57BL/6 mice 1 week after injection were collected and stained with hematoxylin and eosin. Scale bar = 50 μm.

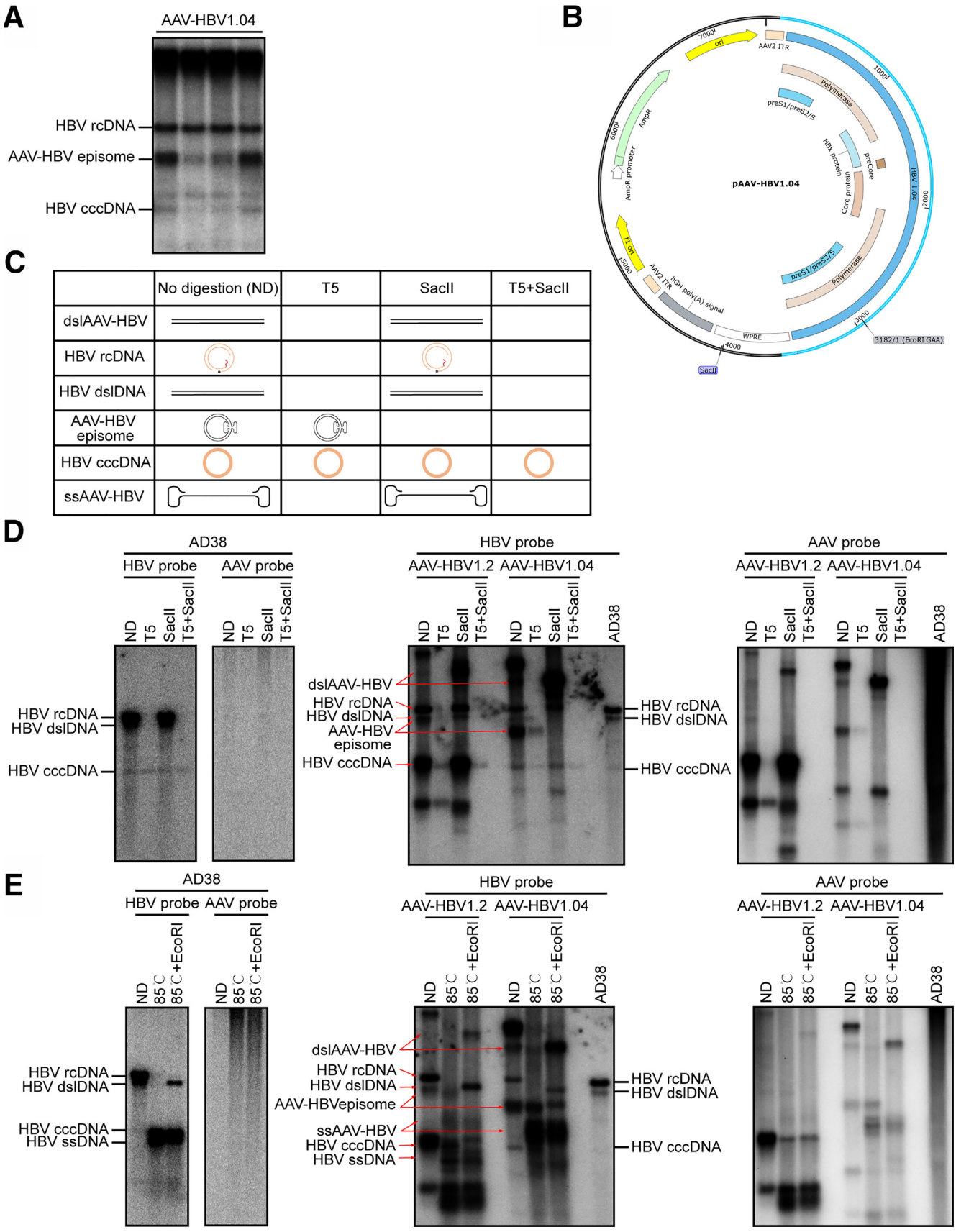
A
AAV-HBV1.04
HBV rcDNA
AAV-HBV episome
HBV cccDNA
B
pAAV-HBV1.04
ori
AAV2 ITR
Polymerase
preS1/preS2/S
HBx protein
preCore
Core protein
HBV 1.04
AmpR
AmpR promoter
f1 ori
AAV2 ITR
hGH poly(A) signal
WPRE
Polymerase
preS1/preS2/S
3182/1 (EcoRI GAA)
SacII
C
No digestion (ND)
T5
SacII
T5+SacII
dslAAV-HBV
HBV rcDNA
HBV dslDNA
AAV-HBV episome
HBV cccDNA
ssAAV-HBV
D
AD38
HBV probe
AAV probe
AAV-HBV1.2
AAV-HBV1.04
ND
T5
SacII
T5+SacII
HBV rcDNA
HBV dslDNA
HBV cccDNA
dslAAV-HBV
AAV-HBV episome
E
85℃
85℃+EcoRI
HBV ssDNA
AAV-HBVepisome
ssAAV-HBV

factor C complex, and DNA ligases.[27–30] In our AAV-HBV1.04 mouse model, treatment of ETV did not interfere with the formation of cccDNA. As ETV blocks reverse transcription it thus restricts synthesis of HBV rcDNA, and this result suggested that cccDNA in this system is originated from AAV-HBV1.04 episome recombination other than rcDNA conversion. In agreement with our conclusion, a recent study showed that HBc-deficient AAV-HBV1.3 still supported cccDNA formation demonstrating that the genesis of cccDNA was independent of HBV replication.[18] By using different DNA damage repair signaling inhibitors, we identified that cccDNA in this model was formed through the ATR pathway. Several kinase family proteins are essential to the DDR. Among them, the ATR protein is responsible primarily for the repair of single-stranded breaks.[31] In particular, ATR plays a vital role in responding to replication stress, which occurs if DNA damage accumulates and impedes the fundamental process of DNA replication.[31] Previous studies demonstrated that AAV replication was able to trigger DDR.[32–34] According to our data, we could speculate that the cccDNA formed in this model was generated by DNA damage signaling kinase ATR-mediated DDR.

In one recent study on an AAV-HBV transduction model, the authors observed that the disappearance of AAV-HBV episome did not result in a significant decline of HBV viral load, which suggests the existence of another HBV replication template.[35] Lucifora *et al*[17] and our study demonstrated that the cccDNA formed from AAV-HBV model is another source of HBV replication.[18] Although it is not converted from rcDNA, the cccDNA in this model is intact and functional. The sequencing data showed that the cccDNA from AAV-HBV1.04 transduction shared identical sequence as wild-type HBV cccDNA. ChIP assays further confirmed the interaction of histone, HBc, and polymerase II with cccDNA, suggesting that the chromatinization and transcriptional regulation of this cccDNA is similar to the cccDNA formed via natural infection.

In previous AAV-HBV1.2 or AAV-HBV1.3 mouse models, all viral proteins can generate from both AAV-HBV episome and cccDNA.[17,18] Thus, the persistence of the AAV-HBV episome will interfere with the analysis of HBV replication markers initiated by cccDNA. As our AAV-HBV1.04 construct itself is HBV replication deficient, the production of HBsAg, viral polymerase, and HBV progeny could only be generated from cccDNA. This model provides a unique platform for studying and developing novel antivirals against HBV cccDNA.

As HBV cccDNA is the key reason for viral persistence, attacking this molecule represents the holy grail to HBV cure. Cell division or direct killing of infected cells by T cells can cause HBV cccDNA loss.[36–38] Additionally, cccDNA destabilizer, cytokine-induced deamination, or gene editing tools can affect the integrity of cccDNA.[39,40] Furthermore, epigenetic drugs may be able to silence cccDNA transcription, resulting in cccDNA inactivation.[41] Because our AAV-HBV1.04 mouse model supports the formation and long-term maintenance of functional cccDNA, it will provide a unique model to dissect the mechanisms of HBV cccDNA maintenance and regulation, as well as for preclinical evaluation of novel therapeutics targeting HBV cccDNA.

Materials And Methods

Construction of Plasmids

The HBV1.04 (3318 bp) and HBV1.2 (3718 bp) DNA fragments were amplified and inserted into AAV vector by ABclonal MultiF Seamless Assembly Mix (RK21020; ABclonal, Wuhan, China). The recombinant plasmids (pAAV-HBV1.04 and pAAV-HBV1.2) contain the 1.04 and 1.2 HBV fragments spanning nucleotides flanked by inverted terminal repeats of AAV, WPRE (woodchuck hepatitis virus posttranscriptional regulatory element), and human growth hormone polyadenylation signal. Primer sequences are listed in Table 1.

Cell Cultures and Transfection

Huh7, HepG2, AML12, HepAD38, and HEK293T cells were maintained in Dulbecco's modified Eagle medium supplemented with 10% fetal bovine serum (Lonsera, Montevideo, Uruguay) and 1% penicillin/streptomycin (Gibco, Waltham, MA). The cell cultures were maintained in a 5% CO_2 atmosphere at 37°C. PEI MAX 40K (PolySciences, Warrington, PA) was used for DNA transfection according to the manufacturer's instructions.

AAV Production and Transduction

HEK293T cells were seeded in 150-mm plate, plasmids (pAAV-HBV1.04 or pAAV-HBV1.2, pAAV2/8-RC, and pHelper in 1:1:1 molar ratio) were cotransfected by using PEI MAX 40K (PolySciences, Warrington, PA). At 72 hours posttransfection, the cell culture supernatants and cells were harvested and filtered with 0.22-μm filter, then concentrated with Amicon Ultra-15 centrifugal filter unit (MilliporeSigma, Burlington, MA). The titer of recombinant AAV was determined by quantitative polymerase chain reaction (qPCR) as described previously.[42] Primer sequences are listed in Table 1.

For AAV-HBV transduction experiments, HepG2 and AML12 cells were seeded in 24-well plates and transduced with 5×10^4 vg per cell diluted in Dulbecco's modified

Figure 5. (***See previous page***). **Characterization of the HBV cccDNA in AAV-HBV1.04–transduced mice.** (*A*) Intrahepatic DNA from AAV-HBV–transduced C57BL/6 mice 1 week posttransduction was extracted following Hirt procedure and subjected to Southern blot analyses using ^{32}P-labeled HBV probes. (*B*) pAAV-HBV1.04 plasmid map. (*C*) Schematic representation of HBV DNA forms extracted by Hirt procedure and their expected behavior after the indicated digestions. (*D*) Intrahepatic DNA from AAV-HBV–transduced C57BL/6 mice at week 1 posttransduction or HepAD38 cells were extracted following Hirt procedure, with or without indicated enzyme digestion, and subjected to Southern blot analyses using ^{32}P labeled HBV or AAV probes. (*E*) Intrahepatic DNA from AAV-HBV–transduced C57BL/6 mice at week 1 posttransduction or HepAD38 cells were extracted following Hirt procedure, and DNA was denatured at 85°C, then treated with EcoRI and subjected to Southern blot analyses using ^{32}P-labeled HBV or AAV probes. ND, none digested. ssDNA, single-stranded DNA.

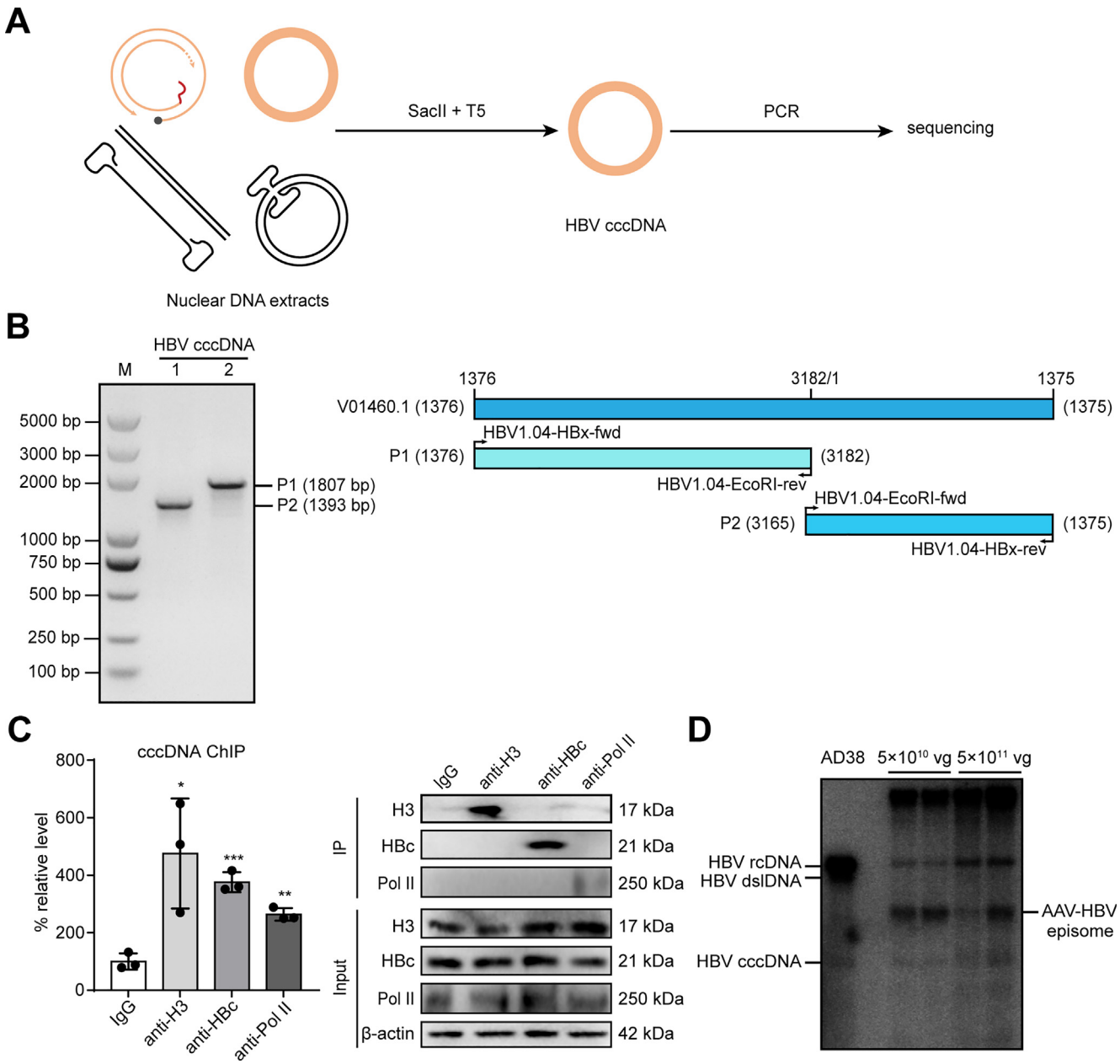

Figure 6. Sequencing of HBV cccDNA and ChIP assays. (*A*) The DNA sample from AAV-HBV1.04–transduced mice were Hirt extracted and both treated with SacII restriction nuclease and T5 exonuclease. (*B*) The remaining HBV cccDNA was used as the template to obtain the fragments of P1 (lane 2, 1807 bp, primers HBV1.04-HBx-fwd and HBV1.04-EcoRI-rev) and P2 (lane 1, 1393 bp, primers HBV1.04-EcoRI-fwd and HBV1.04-HBx-rev) by PCR amplification. An HBV genotype D sequence (GenBank accession no. V01460.1) was used as reference. (*C*) ChIP assays were performed with indicated antibodies or nonspecific IgG antibody control. HBV cccDNA–specific primers were used for qPCR amplification. Samples were normalized to input. (*D*) Intrahepatic DNA from AAV-HBV–transduced C57BL/6 mice at week 44 post-AAV-HBV1.04 transduction was extracted following Hirt procedure and subjected to Southern blot analyses using ^{32}P-labeled HBV probes.

Eagle medium supplemented with 10% fetal bovine serum (Lonsera), 1% penicillin/streptomycin (Gibco), and 4% PEG8000. One day posttransduction, cells were washed 3 times with PBS and treated further as indicated in the following experiment.

Drugs and Inhibitors

Bay 41-4109 racemate (HY-100029A), GLS4 (HY-108917), and ETV (HY-13623) were purchased from MedChemExpress (Monmouth Junction, NJ) and Poly(I:C) (tlr-picw) was purchased from InvivoGen (San Diego, CA). ATM kinase inhibitor (KU-55933), ATR inhibitors (AZD6738, VE-821), and DNA PK inhibitor (KU-57788) were purchased from Selleck Chemicals (Houston, TX).

Mouse Experiments

C57BL/6 mice were purchased from China Three Gorges University Laboratory Animal Center (Yichang, China). Six-

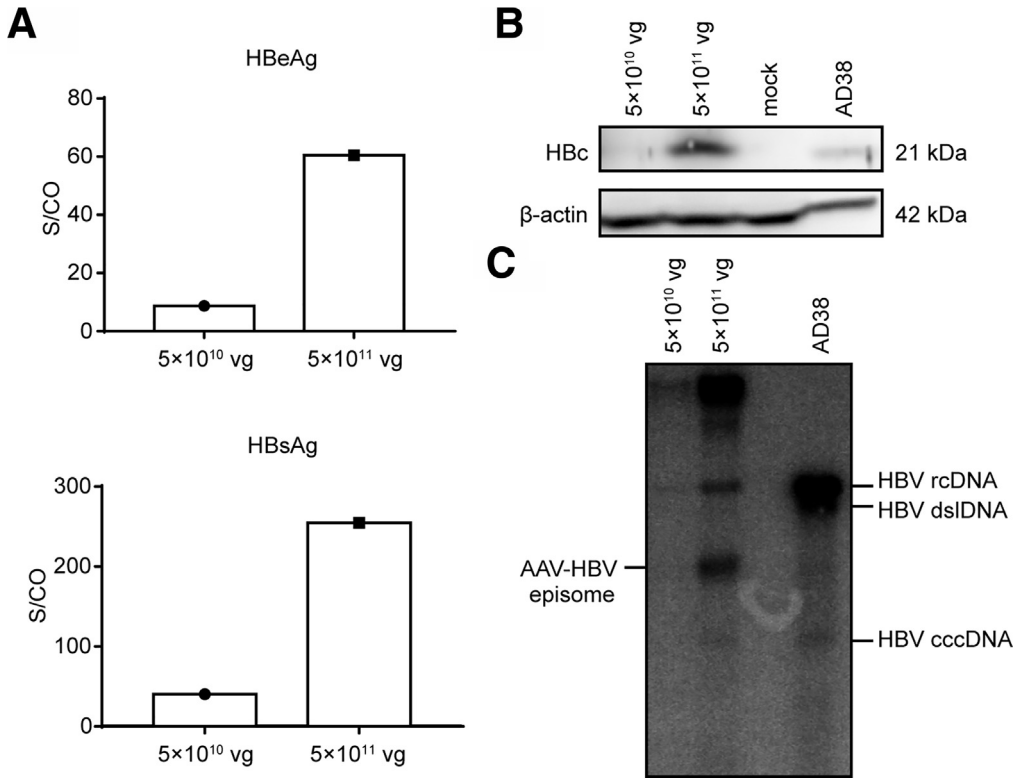

Figure 7. Long-term gene expression and persistence of cccDNA in mouse liver. (*A*) At week 66 post-AAV-HBV1.04 transduction, blood samples were collected for HBeAg and HBsAg testing. (*B*) Liver samples were collected and HBc was tested by Western blot. (*C*) Intrahepatic DNA was extracted following a Hirt procedure and subjected to Southern blot analyses using ^{32}P-labeled HBV probes.

to 8-week-old female mice were used in all experiments. Mice were injected with the recombinant AAV-HBV1.04 (5×10^{10} or 5×10^{11} vg diluted in 200 μL PBS) through tail vein injection as described previously.[42] Blood samples were collected at indicated time points, and serum samples were obtained after centrifugation at 1200 *g* for 15 minutes at 4°C to examine HBV DNA, HBeAg, and HBsAg. The levels of DNA and protein in the liver were determined. The protocol was approved by the Ethic Committee of Animal Facility, Wuhan University.

Analysis of HBV Replication Markers

Secreted HBeAg and HBsAg in culture supernatants were determined by ELISA (Kehua Bio-Engineering, Shanghai, China). Serum HBsAg and HBeAg levels were measured at Renmin Hospital of Wuhan University (Wuhan, China) by electrochemiluminescence immunoassay using the Elecsys HBsAg II and Elecsys HBeAg kits (Roche Diagnostics, Penzberg, Germany) according to the manufacturer's direction. The sample results are presented in the form of a relative cutoff index (signal to cutoff ratio, S/CO). Extracellular HBV DNA was quantified by qPCR using a HBV viral DNA quantitative fluorescence diagnostic kit (Sansure Biotech, Changsha, China), and serum HBV DNA was measured with HBV-DNA real-time qPCR kit (Fosun Diagnostics, Shanghai, China).

Western Blot

Protein samples from cells and mouse liver tissues were obtained by different treatments. The cells were lysed by using lysing buffer (50 mM Tris-HCl [pH 8.0], 5 mM EDTA, 150 mM NaCl, 1% NP-40, 0.1% sodium dodecyl sulfate [SDS]) with protease inhibitor, and 5 mg homogenized liver tissues by Tissue Cell-Destroyer (DS1000; Novastar, Wuhan, China) were suspended in RIPA lysis buffer (Sigma-Aldrich, St Louis, MO) with protease inhibitor, and both were lysed on ice for 30 minutes. The supernatant of cell lysates was collected after centrifugation (4°C, 12,000 *g* for 10 minutes). Then, the protein concentration of the cells and liver tissues was determined using a Bradford Assay Kit (Bio-Rad Laboratories, Hercules, CA) and a BCA Assay Kit (Biosharp, Hefei, China), respectively. In general, 30-μg protein samples were separated by SDS polyacrylamide gel electrophoresis using Mini-PROTEAN Tetra (Bio-Rad Laboratories, Hercules, CA) and transferred into a PVDF membrane (Millipore, Burlington, MA) using a Mini Trans-Blot system (Bio-Rad Laboratories). Following blocked with 5% nonfat milk for 1 hours at room temperature, the membrane was incubated with the primary antibody overnight at 4°C, washed 3 times with Tris-Buffered Saline with Tween, then incubated with secondary antibody. Finally, the signals were detected using Immobilon Western chemiluminescent horseradish peroxidase substrate (Millipore) by a Luminescent Image Analyzer (Syngene, Cambridge, United Kingdom).

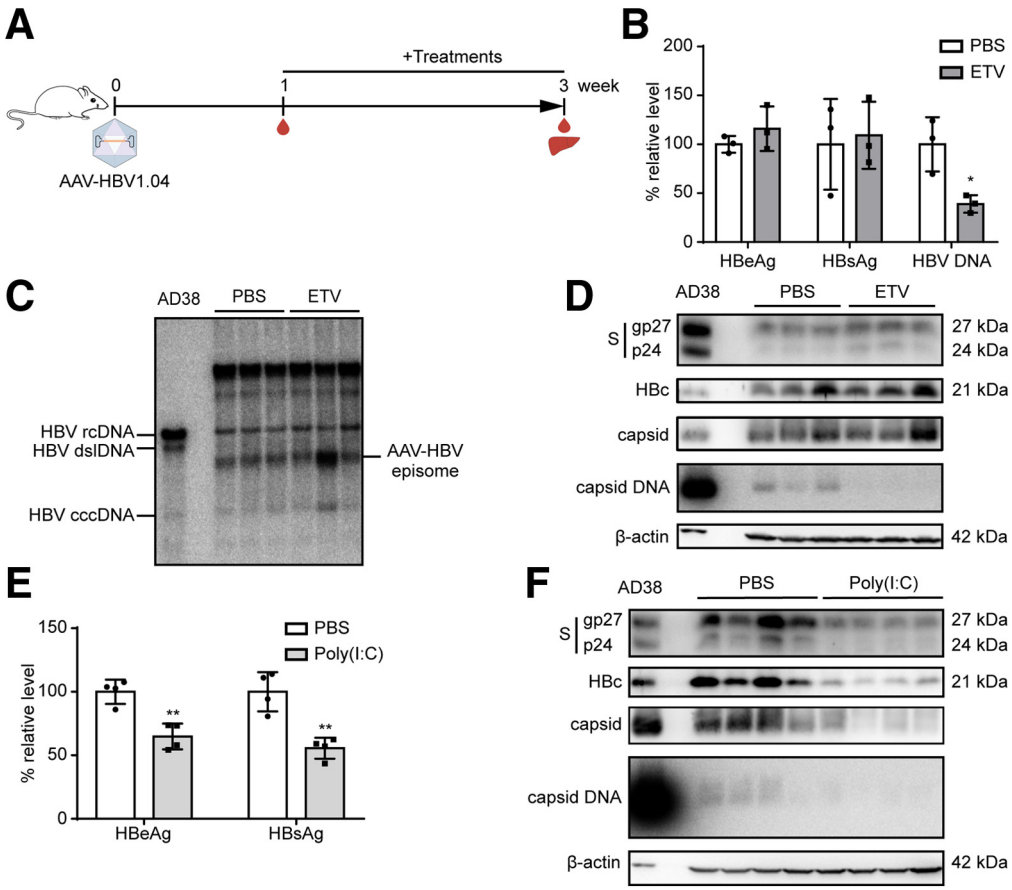

Figure 8. Antiviral response of AAV-HBV1.04–transduced mice. (*A*) One week post-AAV-HBV1.04 injection, different groups of mice were orally dosed with ETV (0.1 mg/kg) (n = 3), or injected intravenously with Poly(I:C) (n = 4, 20 μg/mouse). Two weeks after treatment, all mice were sacrificed for blood and liver samples collection. (*B*) For ETV treatment, the levels of HBsAg, HBeAg, and HBV DNA were determined by ELISA or qPCR, respectively. (*C*) Intrahepatic DNA samples were extracted following Hirt procedure and subjected to Southern blot analyses using ^{32}P-labeled HBV probes. (*D*) Liver samples were collected and lysed, and cell lysates were subjected to Southern blot analysis for encapsidated HBV DNA detection. In addition, Western blot analysis for HBs, HBc, and HBV capsid was performed. (*E*) After Poly(I:C) treatment, the levels of HBsAg and HBeAg were determined by ELISA. (*F*) Liver samples were collected and lysed, and the cell lysates were subjected to Southern blot analysis for encapsidated HBV DNA detection. In addition, Western blot analysis for small S, HBc, and HBV capsid were performed.

Immunofluorescence Staining

Immunofluorescence staining of HBc and HBsAg were performed as described.[42] Briefly, resected mouse liver tissue samples were immediately fixed in 4% paraformaldehyde (Invitrogen, Waltham, MA) for 24 hours, then dehydrated in 40% sucrose solution for 24 hours and embedded in NEG-50 (Thermo Fisher Scientific, Waltham, MA) at −80°C. Liver sections (8-μm thick) were permeabilized with 0.1% Triton X-100 (Sigma-Aldrich) for 10 minutes, 3 times. Slices were then blocked with 10% goat serum (Boster Biological Technology, Wuhan, China) for 1 hour at room temperature, and stained with rabbit anti-HBc (Gene Technology, Shanghai, China) or mouse anti-HBs (S1)[43] overnight at 4°C. Subsequently, samples were incubated with secondary antibody Alexa Fluor 568 goat anti-mouse IgG (Invitrogen) or Alexa Fluor 488 goat anti-rabbit IgG (Invitrogen) for 1 hour at room temperature. The nucleus was stained with Hoechst33258 (Invitrogen) for 5 minutes at room temperature. The images were captured with a confocal laser scanning microscope (Leica, Wetzlar, Germany). More information about the antibodies are listed in Table 2.

Hematoxylin and Eosin Staining

Hematoxylin and eosin staining of mouse liver tissues was by Wuhan Powerful Biology Technology (Wuhan, China) according to the standardized treatment. Briefly, resected mouse liver tissue samples were immediately fixed in 4% paraformaldehyde (Invitrogen) for 24 hours. The tissues were sliced into 5-μm-thick sections, deparaffinized, and stained with hematoxylin and eosin. The staining results were observed under the light microscopy.

Southern Blot

DNA was extracted from cells or 50-mg homogenized liver tissues by Hirt procedure as described previously.[16] DNA samples (cells, 20 μg; liver tissues, 30 μg) were

Table 1. Primer Sequences for PCR and qPCR in This Study

Oligo Name	Sequence Order (5′-3′)
HBV1.04-fwd1	GGCCGCACGCGTGTGTCTAGATTCCTCTTCATCCTGCTGC
HBV1.04-rev1	GGTGGAAGGTTGTGGAATTCCACTGCATGGCCTGAGGATG
HBV1.04-fwd2	GAATTCCACAACCTTCCACC
HBV1.04-rev2	TCGATAACCGGTTTAAAGCTTCAGTAGTCATGCAGGTTCGGC
HBV1.2-fwd1	GGCCGCACGCGTGTGTCTAGACCCGCAAATATACATCGTTTCC
HBV1.2-rev1	GTGGAAAGATTCTGCCCCAT
HBV1.2-fwd2	ATGGGGCAGAATCTTTCCAC
HBV1.2-rev2	TCGATAACCGGTTTAAAGCTTATCTCGTACTGAAGGAAAGAAGTCAG
AAV-HBV-fwd	CTGGGTGGGTGTTAATTTGG
AAV-HBV-rev	TAAGCTGGAGGAGTGCGAAT
cccDNA 92-fwd	GCCTATTGATTGGAAAGTATGT
cccDNA 2251-rev	AGCTGAGGCGGTATCTA
HBV1.04-HBx-fwd	ATGGCTGCTAGGCTGTGCTG
HBV1.04-EcoRI-rev	CCACTGCATGGCCTGAGGAT
HBV1.04-EcoRI-fwd	CCTCAGGCCATGCAGTGGAATTCCACAACCTTCCACCA
HBV1.04-HBx-rev	GGAAACGATGTATATTTGCG

separated by agarose gels, transferred to nylon membrane by capillary siphon method. Then, the nylon membrane was fixed by UV crosslinking and followed by prehybridization, hybridized with probe. Probes were prepared by Random Primer DNA Labeling Kit Ver. 2 (Takara Bio, Shiga, Japan). Finally, the hybridization signal was collected by Typhoon FLA 9500 imager (GE Healthcare Life Sciences, Piscataway, NJ).

Detection of HBV Nucleocapsid and Encapsidated HBV DNA

Detection of HBV nucleocapsid and encapsidated HBV DNA in liver tissue was performed as described previously.[45] Briefly, 20-mg homogenized liver tissues by Tissue Cell-homogenizer (DS1000; Novastar) were suspended in 150 μL lysis buffer (10 mM Tris-HCl [pH 7.5], 50 mM NaCl, 1 mM EDTA, 8% sucrose, and 1% NP-40) and incubated on ice for 10 minutes. The lysate was then centrifuged at 15,800 g for 10 minutes at 4°C. Then 1.2 μL 1 M $MgCl_2$, 4 μL 10 mg/mL DNase I, and 3 μL 100 mg/mL RNase A were added into the supernatant and incubated at 37°C for 20 minutes. The lysate was then centrifuged at 15,800 g for 10 minutes at 4°C. The supernatants were collected and separated by electrophoresis in 1.6% agarose gel. In order to test viral capsid, the agarose gel was directly blotted onto PVDF membranes by capillary blotting. The membranes were blocked with 5% nonfat milk for 1 hour at room temperature then incubated with anti-HBc antibody (Gene Technology) overnight at 4°C. The signals were detected using Immobilon Western chemiluminescent horseradish peroxidase substrate (Millipore) by a Luminescent Image Analyzer (Syngene). In order to detect capsid DNA, the membrane was denatured in denaturation buffer (0.5 M NaOH and 1.5

Table 2. Antibodies Used for Western Blot and Immunostaining

Antibody	Company/Reference	Cat#	Host	Dilution
HBc	Gene Technology	GB058629	Rabbit	1:1000 (Western blot) 1:50 (immunostaining)
HBc	Self-made		Rabbit	1:1000 (Western blot)
β-actin	Cell Signaling Technology	#4970	Rabbit	1:5000 (Western blot)
GAPDH	Proteintech	60004-1-Ig	Mouse	1:1000 (Western blot)
HBs (S1)	Kindly provided by Prof. Xinwen Chen[43]		Mouse	1:50 (immunostaining)
HBsAg	Novus Biologicals	NB100-62652	Rabbit	1:2000 (Western blot)
Histone H3	ABclonal Technology	A2348	Rabbit	1:50 (cccDNA ChIP) 1:1000 (Western blot)
IgG	Cell Signaling Technology	#2729	Rabbit	1:100 (cccDNA ChIP)
RNA polymerase II	Kindly provided by Prof. Kaiwei Liang[44]		Rabbit	1:20 (cccDNA ChIP)
RPB1/POLR2A	Beyotime Biotechnology	AF7788	Rabbit	1:1000 (Western blot)

HBc, hepatitis B virus core protein; HBs, hepatitis B serum; Ig, immunoglobulin;

M NaCl), and neutralized in neutralization buffer (1.5 M NaCl and 1 M Tris-HCl [pH 7.4]). Then, the membrane was fixed by UV crosslinking, prehybridized, and hybridized with DNA probe. Finally, the hybridization signal was collected by Typhoon FLA 9500 imager (GE Healthcare Life Sciences).

ChIP Assay

ChIP assay was performed as described previously.[46] Briefly, 50-mg liver tissues were minced by Tissue Cell-Destroyer (DS1000; Novastar) and homogenized in PBS and fixed in 1% formaldehyde (Invitrogen) for 10 minutes at room temperature, and 1/20 volume of 2.5 M glycine (Sigma-Aldrich) was added to quench formaldehyde. Then, ChIP lysis buffer (50 mM Tris-HCl [pH 8.0], 5 mM EDTA, 150 mM NaCl, 1% NP-40, 0.1% SDS, protease inhibitor) was added and samples were kept on ice for 30 minutes. The lysates were sheared by sonication using a Bioruptor Plus (Diagenode, Seraing, Belgium). Crosslinked chromatin samples were incubated with indicated antibody or normal rabbit immunoglobulin G in a rotator overnight at 4°C. Subsequently, protein A/G-conjugated agarose beads (Smart-Lifesciences, Changzhou, China) were added and incubated in a rotator overnight at 4°C, then the beads were collected and washed 3 times. To elute DNA fragments, immunocomplexes were incubated with elution buffer (50 mM Tris-HCl [pH 8.0], 10 mM EDTA, 1.0% SDS) for 2 hours at 65°C. The elusion was treated with proteinase K (Sigma-Aldrich) overnight at 55°C. Finally, the DNA was purified with a TIANamp Genomic DNA Kit (TIANGEN Biotech, Beijing, China). The purified DNA was detected by qPCR amplification with primers specific for cccDNA. The information of antibodies used is listed in Table 2.

Statistical Analysis

Statistical analysis was performed by GraphPad Prism 7.0 software (GraphPad Software, San Diego, CA). The data presented as the mean ± SD ($n \geq 3$). The statistical analyses were carried out using Student's unpaired 2-tailed t test. P values <.05 were considered significant. $^{*}P < .05$, $^{**}P < .01$, and $^{***}P < .001$.

References

1. Revill PA, Chisari FV, Block JM, Dandri M, Gehring AJ, Guo H, Hu J, Kramvis A, Lampertico P, Janssen HLA, Levrero M, Li W, Liang TJ, Lim SG, Lu F, Penicaud MC, Tavis JE, Thimme R; Members of the ICEHBVWGChairs I-HSG, Advisors I-HS, Zoulim F. A global scientific strategy to cure hepatitis B. Lancet Gastroenterol Hepatol 2019;4:545–558.
2. Polaris Observatory C. Global prevalence, treatment, and prevention of hepatitis B virus infection in 2016: a modelling study. Lancet Gastroenterol Hepatol 2018;3:383–403.
3. Zhao K, Liu A, Xia Y. Insights into hepatitis B virus DNA integration-55 years after virus discovery. Innovation 2020;1:100034.
4. Xia Y, Liang TJ. Development of direct-acting antiviral and host-targeting agents for treatment of hepatitis B virus infection. Gastroenterology 2019;156:311–324.
5. Xia Y, Cheng X, Blossey CK, Wisskirchen K, Esser K, Protzer U. Secreted interferon-inducible factors restrict hepatitis B and C virus entry in vitro. J Immunol Res 2017;2017:4828936.
6. Yan H, Zhong G, Xu G, He W, Jing Z, Gao Z, Huang Y, Qi Y, Peng B, Wang H, Fu L, Song M, Chen P, Gao W, Ren B, Sun Y, Cai T, Feng X, Sui J, Li W. Sodium taurocholate cotransporting polypeptide is a functional receptor for human hepatitis B and D virus. Elife 2012;1:e00049.
7. Guidotti LG, Matzke B, Schaller H, Chisari FV. High-level hepatitis B virus replication in transgenic mice. J Virol 1995;69:6158–6169.
8. Sprinzl MF, Oberwinkler H, Schaller H, Protzer U. Transfer of hepatitis B virus genome by adenovirus vectors into cultured cells and mice: crossing the species barrier. J Virol 2001;75:5108–5118.
9. Dion S, Bourgine M, Godon O, Levillayer F, Michel ML. Adeno-associated virus-mediated gene transfer leads to persistent hepatitis B virus replication in mice expressing HLA-A2 and HLA-DR1 molecules. J Virol 2013;87:5554–5563.
10. Yang PL, Althage A, Chung J, Chisari FV. Hydrodynamic injection of viral DNA: a mouse model of acute hepatitis B virus infection. Proc Natl Acad Sci U S A 2002;99:13825–13830.
11. Dandri M, Burda MR, Torok E, Pollok JM, Iwanska A, Sommer G, Rogiers X, Rogler CE, Gupta S, Will H, Greten H, Petersen J. Repopulation of mouse liver with human hepatocytes and in vivo infection with hepatitis B virus. Hepatology 2001;33:981–988.
12. Yuan L, Jiang J, Liu X, Zhang Y, Zhang L, Xin J, Wu K, Li X, Cao J, Guo X, Shi D, Li J, Jiang L, Sun S, Wang T, Hou W, Zhang T, Zhu H, Zhang J, Yuan Q, Cheng T, Li J, Xia N. HBV infection-induced liver cirrhosis development in dual-humanised mice with human bone mesenchymal stem cell transplantation. Gut 2019;68:2044–2056.
13. Qi Z, Li G, Hu H, Yang C, Zhang X, Leng Q, Xie Y, Yu D, Zhang X, Gao Y, Lan K, Deng Q. Recombinant covalently closed circular hepatitis B virus DNA induces prolonged viral persistence in immunocompetent mice. J Virol 2014;88:8045–8056.
14. Li G, Zhu Y, Shao D, Chang H, Zhang X, Zhou D, Gao Y, Lan K, Deng Q. Recombinant covalently closed circular DNA of hepatitis B virus induces long-term viral persistence with chronic hepatitis in a mouse model. Hepatology 2018;67:56–70.
15. Wu M, Wang C, Shi B, Fang Z, Qin B, Zhou X, Zhang X, Yuan Z. A novel recombinant cccDNA-based mouse model with long term maintenance of rcccDNA and antigenemia. Antiviral Res 2020;180:104826.
16. Yan Z, Zeng J, Yu Y, Xiang K, Hu H, Zhou X, Gu L, Wang L, Zhao J, Young JAT, Gao L. HBVcircle: a novel tool to investigate hepatitis B virus covalently closed circular DNA. J Hepatol 2017;66:1149–1157.
17. Lucifora J, Salvetti A, Marniquet X, Mailly L, Testoni B, Fusil F, Inchauspe A, Michelet M, Michel ML, Levrero M,

Cortez P, Baumert TF, Cosset FL, Challier C, Zoulim F, Durantel D. Detection of the hepatitis B virus (HBV) covalently-closed-circular DNA (cccDNA) in mice transduced with a recombinant AAV-HBV vector. Antiviral Res 2017;145:14–19.
18. Ko C, Su J, Festag J, Bester R, Kosinska AD, Protzer U. Intramolecular recombination enables the formation of hepatitis B virus (HBV) cccDNA in mice after HBV genome transfer using recombinant AAV vectors. Antiviral Res 2021;194:105140.
19. Collaco RF, Bevington JM, Bhrigu V, Kalman-Maltese V, Trempe JP. Adeno-associated virus and adenovirus coinfection induces a cellular DNA damage and repair response via redundant phosphatidylinositol 3-like kinase pathways. Virology 2009;392:24–33.
20. Lok AS, Zoulim F, Dusheiko G, Ghany MG. Hepatitis B cure: from discovery to regulatory approval. Hepatology 2017;66:1296–1313.
21. Laras A, Koskinas J, Dimou E, Kostamena A, Hadziyannis SJ. Intrahepatic levels and replicative activity of covalently closed circular hepatitis B virus DNA in chronically infected patients. Hepatology 2006; 44:694–702.
22. Wieland SF. The chimpanzee model for hepatitis B virus infection. Cold Spring Harb Perspect Med 2015; 5:a021469.
23. Walter E, Keist R, Niederöst B, Pult I, Blum HE. Hepatitis B virus infection of tupaia hepatocytes in vitro and in vivo. Hepatology 1996;24:1–5.
24. Yan H, Peng B, He W, Zhong G, Qi Y, Ren B, Gao Z, Jing Z, Song M, Xu G, Sui J, Li W. Molecular determinants of hepatitis B and D virus entry restriction in mouse sodium taurocholate cotransporting polypeptide. J Virol 2013;87:7977–7991.
25. Lempp FA, Mutz P, Lipps C, Wirth D, Bartenschlager R, Urban S. Evidence that hepatitis B virus replication in mouse cells is limited by the lack of a host cell dependency factor. J Hepatol 2016;64:556–564.
26. Xia Y, Guo H. Hepatitis B virus cccDNA: Formation, regulation and therapeutic potential. Antiviral Res 2020; 180:104824.
27. Kitamura K, Que L, Shimadu M, Koura M, Ishihara Y, Wakae K, Nakamura T, Watashi K, Wakita T, Muramatsu M. Flap endonuclease 1 is involved in cccDNA formation in the hepatitis B virus. PLoS Pathog 2018;14:e1007124.
28. Qi Y, Gao Z, Xu G, Peng B, Liu C, Yan H, Yao Q, Sun G, Liu Y, Tang D, Song Z, He W, Sun Y, Guo JT, Li W. DNA Polymerase kappa is a key cellular factor for the formation of covalently closed circular DNA of hepatitis B virus. PLoS Pathog 2016;12:e1005893.
29. Long Q, Yan R, Hu J, Cai D, Mitra B, Kim ES, Marchetti A, Zhang H, Wang S, Liu Y, Huang A, Guo H. The role of host DNA ligases in hepadnavirus covalently closed circular DNA formation. PLoS Pathog 2017;13:e1006784.
30. Wei L, Ploss A. Core components of DNA lagging strand synthesis machinery are essential for hepatitis B virus cccDNA formation. Nat Microbiol 2020;5:715–726.
31. Liu S, Opiyo SO, Manthey K, Glanzer JG, Ashley AK, Amerin C, Troksa K, Shrivastav M, Nickoloff JA, Oakley GG. Distinct roles for DNA-PK, ATM and ATR in RPA phosphorylation and checkpoint activation in response to replication stress. Nucleic Acids Res 2012; 40:10780–10794.
32. Schwartz RA, Carson CT, Schuberth C, Weitzman MD. Adeno-associated virus replication induces a DNA damage response coordinated by DNA-dependent protein kinase. J Virol 2009;83:6269–6278.
33. Cataldi MP, McCarty DM. Differential effects of DNA double-strand break repair pathways on single-strand and self-complementary adeno-associated virus vector genomes. J Virol 2010;84:8673–8682.
34. Jurvansuu J, Fragkos M, Ingemarsdotter C, Beard P. Chk1 instability is coupled to mitotic cell death of p53-deficient cells in response to virus-induced DNA damage signaling. J Mol Biol 2007;372:397–406.
35. Suarez-Amaran L, Usai C, Di Scala M, Godoy C, Ni Y, Hommel M, Palomo L, Segura V, Olague C, Vales A, Ruiz-Ripa A, Buti M, Salido E, Prieto J, Urban S, Rodriguez-Frias F, Aldabe R, Gonzalez-Aseguinolaza G. A new HDV mouse model identifies mitochondrial antiviral signaling protein (MAVS) as a key player in IFN-beta induction. J Hepatol 2017;67:669–679.
36. Allweiss L, Volz T, Giersch K, Kah J, Raffa G, Petersen J, Lohse AW, Beninati C, Pollicino T, Urban S, Lutgehetmann M, Dandri M. Proliferation of primary human hepatocytes and prevention of hepatitis B virus reinfection efficiently deplete nuclear cccDNA in vivo. Gut 2018;67:542–552.
37. Bohne F, Chmielewski M, Ebert G, Wiegmann K, Kurschner T, Schulze A, Urban S, Kronke M, Abken H, Protzer U. T cells redirected against hepatitis B virus surface proteins eliminate infected hepatocytes. Gastroenterology 2008;134:239–247.
38. Xia Y, Stadler D, Lucifora J, Reisinger F, Webb D, Hösel M, Michler T, Wisskirchen K, Cheng X, Zhang K, Chou WM, Wettengel JM, Malo A, Bohne F, Hoffmann D, Eyer F, Thimme R, Falk CS, Thasler WE, Heikenwalder M, Protzer U. Interferon-γ and tumor necrosis factor-α produced by T cells reduce the HBV persistence form, cccDNA, without cytolysis. Gastroenterology 2016;150:194–205.
39. Lucifora J, Xia Y, Reisinger F, Zhang K, Stadler D, Cheng X, Sprinzl MF, Koppensteiner H, Makowska Z, Volz T, Remouchamps C, Chou WM, Thasler WE, Huser N, Durantel D, Liang TJ, Munk C, Heim MH, Browning JL, Dejardin E, Dandri M, Schindler M, Heikenwalder M, Protzer U. Specific and nonhepatotoxic degradation of nuclear hepatitis B virus cccDNA. Science 2014;343:1221–1228.
40. Koh S, Kah J, Tham CYL, Yang N, Ceccarello E, Chia A, Chen M, Khakpoor A, Pavesi A, Tan AT, Dandri M, Bertoletti A. Nonlytic lymphocytes engineered to express virus-specific T-cell receptors limit HBV infection by activating APOBEC3. Gastroenterology 2018;155:180–193.e6.
41. Gilmore S, Tam D, Dick R, Appleby T, Birkus G, Willkom M, Delaney WE, Notte GT, Feierbach B. Antiviral activity of GS-5801, a liver-targeted prodrug of a lysine demethylase 5 inhibitor, in a hepatitis B virus primary human hepatocyte infection model. J Hepatol 2017;66:2.

42. Teng Y, Xu Z, Zhao K, Zhong Y, Wang J, Zhao L, Zheng Z, Hou W, Zhu C, Chen X, Protzer U, Li Y, Xia Y. Novel function of SART1 in HNF4alpha transcriptional regulation contributes to its antiviral role during HBV infection. J Hepatol 2021;75:1072–1082.
43. Cao L, Wu C, Shi H, Gong Z, Zhang E, Wang H, Zhao K, Liu S, Li S, Gao X, Wang Y, Pei R, Lu M, Chen X. Coexistence of hepatitis B virus quasispecies enhances viral replication and the ability to induce host antibody and cellular immune responses. J Virol 2014;88:8656–8666.
44. Liang K, Woodfin AR, Slaughter BD, Unruh JR, Box AC, Rickels RA, Gao X, Haug JS, Jaspersen SL, Shilatifard A. Mitotic transcriptional activation: clearance of actively engaged Pol II via transcriptional elongation control in mitosis. Mol Cell 2015;60:435–445.
45. Zhang S, Guo JT, Wu JZ, Yang G. Identification and characterization of multiple TRIM proteins that inhibit hepatitis B virus transcription. PLoS One 2013;8:e70001.
46. Lee TI, Johnstone SE, Young RA. Chromatin immunoprecipitation and microarray-based analysis of protein location. Nat Protoc 2006;1:729–748.

Received July 14, 2021. Accepted November 30, 2021.

Correspondence
Address correspondence to: Yuchen Xia, PhD, Institute of Medical Virology, School of Basic Medical Sciences, Wuhan University, Wuhan, Hubei 430071, China. e-mail: yuchenxia@whu.edu.cn; fax: 0086-27-68759222.

Acknowledgments
The authors thank Mr. Cong Li and the staffs at the Research Center for Medicine and Structural Biology of Wuhan University for technical assistance.

CRediT Authorship Contributions
Zaichao Xu, MSc (Investigation: Equal; Methodology: Equal; Validation: Lead; Writing – original draft: Supporting; Writing – review & editing: Equal)
Li Zhao, MSc (Investigation: Equal; Methodology: Equal; Validation: Equal; Writing – review & editing: Supporting)
Youquan Zhong, Mr (Investigation: Equal; Methodology: Equal; Writing – review & editing: Supporting)
Chengliang Zhu, PhD (Investigation: Equal; Writing – review & editing: Supporting)
Kaitao Zhao, PhD (Investigation: Supporting; Writing – review & editing: Supporting)
Yan Teng, MSc (Investigation: Supporting; Writing – review & editing: Supporting)
Xiaoming Cheng (Formal analysis: Supporting; Validation: Supporting; Writing – review & editing: Supporting)
Qiang Chen, PhD (Formal analysis: Supporting; Resources: Supporting; Writing – review & editing: Supporting)
Yuchen Xia, Ph.D (Conceptualization: Lead; Funding acquisition: Lead; Supervision: Lead; Writing – original draft: Lead; Writing – review & editing: Lead)

Conflicts of interest
The authors disclose no conflicts.

Funding
This work was supported by the National Natural Science Foundation of China (project no. 81971936), the Fundamental Research Funds for the Central Universities, Hubei Province's Outstanding Medical Academic Leader Program, the Gilead Sciences Research Scholars Program in Liver Disease Asia, the Foundation for Innovative Research Groups of the Natural Science Foundation of Hubei (project no. 2020CFA015), and the Research and Innovation Team Project of Hubei Health Commission (project no. WJ2021C002).